
PERGAMON

Journal of the Mechanics and Physics of Solids
51 (2003) 1413–1431

JOURNAL OF THE
MECHANICS AND
PHYSICS OF SOLIDS

www.elsevier.com/locate/jmps

Theoretical and experimental analysis of longitudinal wave propagation in cylindrical viscoelastic rods

A. Benatar[a], D. Rittel[b,*], A.L. Yarin[b]

[a] *Department of Industrial, Welding and Systems Engineering, The Ohio State University, 1248 Arthur E. Adams Drive, Columbus, OH 43221-3560, USA*
[b] *Department of Mechanical Engineering, Faculty of Mechanical Engineering, Israel Institute of Technology, Technion, Haifa 32000, Israel*

Received 13 March 2003; accepted 26 March 2003

Abstract

Wave propagation in viscoelastic rods is encountered in many applications including studies of impact and fracture under high strain rates and characterization of the dynamic behavior of viscoelastic materials. For viscoelastic materials, both material and geometric dispersion are possible when the diameter of the rod is of the same order as the wavelength. In this work, we simplify the Pochhammer frequency equation for low and intermediate loss viscoelastic materials and formulate corrections for geometric dispersion for both the phase velocity and attenuation. The formulation is then experimentally verified with measurements of the phase velocity and attenuation in commercial polymethylmethacrylate rods that are 12 and 6.4 mm in diameter. Without correcting for geometric dispersion, the usable frequency range for determining the phase velocity and attenuation for the 12 mm rod is about 20 kHz, and about 35 kHz for the 6.4 mm rod. Using the correction procedure developed here, it was possible to accurately determine the phase velocity and attenuation up to frequencies exceeding 55 kHz for the 12 mm rod and 65 kHz for the 6.4 mm rod. These corrections are applicable to many polymers and other viscoelastic materials. From thereon, the viscoelastic properties of the material can be determined over a wide range of frequencies.

Keywords: Wave propagation; Viscoelastic; Correction for geometric dispersion; Cylindrical rods

* Corresponding author. Tel.: +972-4-8293261; fax: 974-4-8295711.
E-mail address: merittel@tx.technion.ac.il (D. Rittel).

0022-5096/03/$ - see front matter © 2003 Elsevier Science Ltd. All rights reserved.
doi:10.1016/S0022-5096(03)00056-5

1. Introduction

Wave propagation in viscoelastic rods is encountered in many applications including studies of impact and fracture under high strain rates and characterization of the dynamic behavior of viscoelastic materials. For viscoelastic materials, the phase velocity increases with increasing frequency. Therefore, when a strain pulse propagates along a viscoelastic rod, high-frequency components propagate faster than low-frequency components resulting in dispersion of the pulse (Kolsky, 1956). This phenomenon is often referred to as viscoelastic dispersion or as material dispersion. In addition, for frequencies where the wavelength is of the same order as the diameter of the rod, geometric dispersion occurs (see Kolsky, 1963). Therefore, both geometric and material dispersion are possible in viscoelastic rods. Since the analysis of the geometric dispersion in viscoelastic rods is not well developed, great care is taken to insure that one-dimensional analysis is sufficiently accurate for practical purposes. Generally, this requires the use of small diameter rods and limits the usable frequency range so that the wavelength is always much greater than the diameter of the rod.

Pochhammer (1876) and Chree (1889) formulated the equations and solutions for wave propagation in semi-infinite elastic cylindrical rods. For longitudinal waves, imposing the boundary condition of zero stress at the outer surface of the rod results in the Pochhammer frequency equation. Bancroft (1941) was the first to study the lowest branch (mode) of the roots of the Pochhammer frequency equation and to evaluate the relation between the phase velocity and the wavenumber. Hudson (1943) later reaffirmed many of Bancroft's results and showed that there is one point on the lower branch that is invariant to changes in Poisson's ratio. Davis (1948) performed an extensive theoretical and experimental study of the propagation of sharp pulses in cylindrical rods. He showed that the Pochhammer and Chree solutions are not exact for a finite length rod but are sufficiently close to the exact ones in most cases. He also showed that in addition to dispersion, the effect of lateral inertia is to smooth the base of the reflected pulse with very slight oscillations being predicted. Onoe et al. (1962) performed an in-depth study of the Pochhammer frequency equation resulting in a wide frequency spectrum relating the phase velocity to the wavenumber for many modes or branches.

Most experimental and theoretical studies on the propagation of waves and pulses in viscoelastic rods were limited to 1-D cases, so that geometric dispersion could be neglected. Kolsky (1956, 1976) was one of the first to study the propagation of short mechanical pulses along polymeric rods. Assuming 1-D analysis, he used the shape of the pulses to determine the phase velocity and attenuation as a function of frequency. Lundberg and Blanc (1988), Blanc (1993), described the use of transient pulses and Fourier transform techniques to measure the phase velocity and attenuation as a function of frequency. The storage and loss moduli of the polymer were then determined from the phase velocity and attenuation using 1-D wave propagation solutions.

In many instances, especially when considering higher frequencies, 1-D solutions are not suitable because the wavelength at the higher frequencies can be of the same order or smaller than the diameter of the rod. Coquin (1964) developed the governing equations and solutions for harmonic wave propagation in an infinite Voigt solid.

Unfortunately, as shown by Kolsky (1956), neither Voigt nor Maxwell material models can adequately describe the behavior of real polymers. Zhao and Gary (1995) extended the Pochhammer (1876) and Chree (1889) solutions for elastic cylindrical rods to viscoelastic rods. They showed that, by considering propagation of harmonic waves in an infinite cylindrical rod in the frequency domain through the use of the Fourier transform, the solution is identical to the elastic solution except that the modulus is complex. Similarly, the frequency equation for the viscoelastic material is identical to the elastic case except that the parameters become complex. Zhao and Gary (1995) suggested that the viscoelastic frequency equation could not be used to correct for geometric dispersion without prior knowledge of the corrected moduli. Therefore, they proposed correcting for geometric dispersion empirically. They also gave an empirical relation limiting the maximum frequency of measurement for a specific rod diameter and error level. Bacon (1998) adopted a purely experimental approach to correct for both material dispersion and geometric dispersion in Hopkinson bar type experiments. He showed that for polymethylmethacrylate (PMMA) bars that are 40 mm in diameter, geometric dispersion becomes significant at frequencies exceeding 5 kHz. He suggested the use of the experimentally measured propagation coefficient, which includes material and geometric dispersion, for any future corrections with the same rod. However, this approach does not provide a priori correction for materials with unknown moduli, nor does it enable characterization of the mechanical behavior of the viscoelastic material at high frequencies. Additional experimental work aimed at identifying viscoelastic properties can be found in the work of Sogabe and Kishida (1982) and Sogabe and Tsuzuki (1986) on polymers and metals, as well as in Hillstrom et al. (2000) on various polymers. These works are within the 1-D framework, and the highest investigated frequency does not exceed 10 KHz.

In this work, the Pochhammer frequency equation is simplified for low to intermediate loss viscoelastic rods. The simplified frequency equation is then used to develop corrections for geometric dispersion in the phase velocity and attenuation. These corrections are next applied to experimental measurements of the phase velocity and attenuation in commercial PMMA over a wide range of frequencies.

2. Theory

2.1. Pochhammer frequency equation for viscoelastic rods

Zhao and Gary (1995) derived the solution for wave propagation in axisymmetric viscoelastic rods in the frequency domain. They also derived Pochhammer frequency equation for viscoelastic rods, giving

$$\frac{2p}{a}(q^2+k^2)J_1(pa)J_1(qa)-(q^2-k^2)^2J_0(pa)J_1(qa) - 4k^2pqJ_1(pa)J_0(qa)=0, \tag{1}$$

where a is the radius of the rod, and $J_0(z)$ and $J_1(z)$ are the Bessel functions of the first kind and zero and first order, respectively. The following relations define the

remaining parameters in the Pochhammer frequency equation (see Achenbach, 1987; Graff, 1975):

$$p^2 = \frac{\omega^2}{c_L^2} - k^2 = \frac{\rho\omega^2}{\lambda^* + 2\mu^*} - k^2 = \frac{\rho s_1^2 \omega^2}{E^*} - k^2, \tag{2}$$

$$q^2 = \frac{\omega^2}{c_T^2} - k^2 = \frac{\rho\omega^2}{\mu^*} - k^2 = \frac{\rho s_2^2 \omega^2}{E^*} - k^2, \tag{3}$$

$$s_1 = \sqrt{\frac{(1+\nu)(1-2\nu)}{(1-\nu)}}, \tag{4}$$

$$s_2 = \sqrt{2(1+\nu)}, \tag{5}$$

where c_L is the complex dilatational wave velocity, c_T is the complex shear wave velocity, ω is the radial frequency, λ^* and μ^* are the complex Lamé constants, ρ is the density, E^* is the complex Young's modulus, ν is the Poisson's ratio (assumed real as discussed later), and k is the complex wavenumber. Therefore, the Pochhammer frequency equation for viscoelastic rods is identical to that of elastic rods except that the parameters are complex.

Just like in the case of the elastic material, the Pochhammer frequency equation can be used to describe and correct for the geometric dispersion in viscoelastic rods. The difficulty is that the parameters in Eq. (1) are complex, making its use more difficult. According to Zhao and Gary (1995), it is necessary to know the viscoelastic properties of the rod in order to correct for geometric dispersion using Eq. (1). However, if these properties are already known, it is usually not necessary to correct for dispersion anymore. Therefore, they propose an iterative approach along with an empirical relation to determine the maximum critical frequency for which 1-D analysis is accurate to within 5%.

2.2. The simplified Pochhammer frequency equation for low loss viscoelastic rods

In the case of low loss viscoelastic materials it is possible to simplify the Pochhammer frequency equation so that corrections for geometric dispersion can be easily done. The complex modulus for a viscoelastic material can be written in terms of the real (storage, E') and imaginary (loss, E'') components as follows (Christensen, 1982):

$$E^* = E' + \mathrm{i}E''. \tag{6}$$

The loss tangent is defined as follows:

$$\tan\delta = \frac{E''}{E'}. \tag{7}$$

For a low loss viscoelastic material ($\tan\delta \ll 1$), it is possible to approximate the loss tangent and complex modulus as follows:

$$\delta \approx \tan\delta = \frac{E''}{E'}, \tag{8}$$

$$E^* \approx E'(1 + \mathrm{i}\delta). \tag{9}$$

First, the low loss viscoelastic material approximation can be used in the case of a *slender bar*, where the 1-D equations can be used. The wavenumber, k_b, can be written in this case as follows:

$$k_\mathrm{b} = \frac{\omega}{c_\mathrm{b}} \approx \frac{\omega}{c_0} - \mathrm{i}\alpha_0 = \omega\sqrt{\frac{\rho}{E^*}} \approx \frac{\omega\sqrt{\rho}}{\sqrt{E'(1+\mathrm{i}\delta)}} \approx \omega\sqrt{\frac{\rho}{E}}\left(1 - \frac{\mathrm{i}\delta}{2}\right), \tag{10}$$

where c_b is the complex longitudinal bar wave velocity, and

$$c_0 = \sqrt{\frac{E'}{\rho}} \quad \text{and} \quad \alpha_0 = \omega\frac{\delta}{2}\sqrt{\frac{\rho}{E'}}. \tag{11}$$

Eq. (10) can also be written in the following form:

$$k_\mathrm{b} \approx k'_\mathrm{b}(1 - \mathrm{i}\delta_\mathrm{b}), \tag{12}$$

where $k'_\mathrm{b} = \omega\sqrt{\frac{\rho}{E'}}$ and $\delta_\mathrm{b} = \frac{\delta}{2}$.

Consider now a *cylindrical viscoelastic rod*. By rod, it is meant that the bar has a finite cross section, with displacements in the longitudinal and radial directions. The wavenumber of such a rod, with or without geometric dispersion, is assumed to be of the same magnitude as the wavenumber of a slender bar.

Therefore, similar to Eq. (12), for any low loss ($\delta_k \ll 1$) viscoelastic cylindrical rod one can write the wavenumber in the following generic form:

$$k \approx k'(1 - \mathrm{i}\delta_k). \tag{13}$$

Next, consider the other terms in the Pochhammer frequency equation (Eq. (1)). From Eqs. (2) and (3), the dilatational and shear wave velocities can be expressed in terms of the longitudinal bar wave velocity as shown below:

$$c_\mathrm{L} = \frac{c_\mathrm{b}}{s_1}, \tag{14}$$

$$c_\mathrm{T} = \frac{c_\mathrm{b}}{s_2}. \tag{15}$$

For viscoelastic materials that are subjected to loadings for short times or at high frequency, it is reasonable to assume that Poisson's ratio is real, and that its value would be substantially less than the value of 0.5 for incompressible solids (the minimum value ordinarily observed for homogeneous and isotropic materials is about 0.2, see e.g., Ferry, 1980). Combining Eqs. (2), (10)–(14), one gets

$$p^2 = \frac{\omega^2 s_1^2}{c_\mathrm{b}^2} - k^2 \approx s_1^2 k_\mathrm{b}'^2(1 - 2\mathrm{i}\delta_\mathrm{b}) - k'^2(1 - 2\mathrm{i}\delta_k). \tag{16}$$

Therefore,

$$p^2 \approx p'^2(1 - 2\mathrm{i}\delta_p), \tag{17}$$

where

$$p'^2 = s_1^2 k_\mathrm{b}'^2 - k'^2, \tag{18}$$

$$\delta_p = \frac{s_1^2 k_\mathrm{b}'^2 \delta_\mathrm{b} - k'^2 \delta_k}{s_1^2 k_\mathrm{b}'^2 - k'^2}. \tag{19}$$

Similarly, combining Eqs. (3), (10), (12), (13) and (15) gives

$$q^2 = \frac{\omega^2 s_2^2}{c_\mathrm{b}^2} - k^2 \approx s_2^2 k_\mathrm{b}'^2(1 - 2\mathrm{i}\delta_\mathrm{b}) - k'^2(1 - 2\mathrm{i}\delta_k). \tag{20}$$

As a result we obtain

$$q^2 \approx q'^2(1 - 2\mathrm{i}\delta_q), \tag{21}$$

where

$$q'^2 = s_2^2 k_\mathrm{b}'^2 - k'^2, \tag{22}$$

$$\delta_q = \frac{s_2^2 k_\mathrm{b}'^2 \delta_\mathrm{b} - k'^2 \delta_k}{s_2^2 k_\mathrm{b}'^2 - k'^2}. \tag{23}$$

Substituting the approximate expressions for p (Eq. (17)) and q (Eq. (21)) into the Pochhammer frequency equation (Eq. (1)) yields

$$\begin{aligned}
&\frac{2p'(1 - \mathrm{i}\delta_p)}{a}(q'^2(1 - 2\mathrm{i}\delta_q) + k'^2(1 - 2\mathrm{i}\delta_k))J_1(p'(1 - \mathrm{i}\delta_p)a)J_1(q'(1 - \mathrm{i}\delta_q)a) \\
&-(q'^2(1 - 2\mathrm{i}\delta_q) - k'^2(1 - 2\mathrm{i}\delta_k))^2 J_0(p'(1 - \mathrm{i}\delta_p)a)J_1(q'(1 - \mathrm{i}\delta_q)a) \\
&- 4k'^2(1 - 2\mathrm{i}\delta_k)p'(1 - \mathrm{i}\delta_p)q'(1 - \mathrm{i}\delta_q)J_1(p'(1 - \mathrm{i}\delta_p)a)J_0(q'(1 - \mathrm{i}\delta_q)a) = 0
\end{aligned} \tag{24}$$

To simplify Eq. (24) further, it is necessary to simplify the Bessel functions for arguments of the following form $x = x'(1 - \mathrm{i}\delta_x)$, where $\delta_x \ll 1$.

Using the definition of the Bessel functions as a series (Hildebrand, 1976), one shows that

$$J_n(x'(1 - \mathrm{i}\delta_x)) \approx J_n(x') - \mathrm{i}\delta_x(x'J_{n-1}(x') - nJ_n(x')). \tag{25}$$

In particular, from Eq. (25), we obtain

$$J_0(x'(1 - \mathrm{i}\delta_x)) \approx J_0(x') + \mathrm{i}x'\delta_x J_1(x'), \tag{26}$$

$$J_1(x'(1 - \mathrm{i}\delta_x)) \approx J_1(x') - \mathrm{i}\delta_x(x'J_0(x') - J_1(x')). \tag{27}$$

Denoting $\bar{p}' = p'a, \bar{q}' = q'a$ and $\bar{k}' = k'a$, and using Eqs. (26) and (27), we obtain the following linearized *real* part from Eq. (24):

$$2\bar{p}'(\bar{q}'^2 + \bar{k}'^2)J_1(\bar{p}')J_1(\bar{q}') - (\bar{q}'^2 - \bar{k}'^2)^2 J_0(\bar{p}')J_1(\bar{q}') - 4\bar{k}'^2\bar{p}'\bar{q}'J_1(\bar{p}')J_0(\bar{q}') = 0, \tag{28}$$

and the linearized *imaginary* part of Eq. (24) reads

$$\begin{aligned}
&2\delta_q\bar{k}'^2\bar{p}'J_1(\bar{q}')J_1(\bar{p}') - 2\delta_q\bar{p}'J_1(\bar{p}')(\bar{q}'^3J_0(\bar{q}') + \bar{q}'^2J_1(\bar{q}')) \\
&- 2\delta_p\bar{p}'^2J_0(\bar{p}')J_1(\bar{q}')(\bar{q}'^2 + \bar{k}'^2) - 4\delta_k\bar{p}'\bar{k}'^2J_1(\bar{p}')J_1(\bar{q}') \\
&+ \delta_q J_0(\bar{p}')(3\bar{q}'^4J_1(\bar{q}') - 2\bar{q}'^3\bar{k}'^2J_0(\bar{q}') - 2\bar{q}'^2\bar{k}'^2J_1(\bar{q}') + \bar{q}'\bar{k}'^4J_0(\bar{q}')) \\
&- \delta_q J_0(\bar{p}')(\bar{k}'^4J_1(\bar{q}') - \bar{q}'^5J_0(\bar{q}')) + \delta_p\bar{p}'J_1(\bar{q}')J_1(\bar{p}')(\bar{q}'^4 + \bar{k}'^4 - 2\bar{q}'^2\bar{k}'^2) \\
&- 4\delta_k\bar{k}'^2J_1(\bar{q}')J_0(\bar{p}')(\bar{q}'^2 - \bar{k}'^2) - 4\delta_q\bar{p}'\bar{q}'\bar{k}'^2J_1(\bar{p}')(\bar{q}'J_1(\bar{q}') + 1/2(J_0(\bar{q}'))) \\
&+ 4\delta_p\bar{q}'\bar{p}'^2\bar{k}'^2J_0(\bar{p}')J_0(\bar{q}') + 8\delta_k\bar{p}'\bar{q}'\bar{k}'^2J_1(\bar{p}')J_0(\bar{q}') = 0.
\end{aligned} \tag{29}$$

Eq. (28) is identical to the Pochhammer frequency equation for elastic materials. It is expressed solely in terms of *real parts of the parameters*. Like in the purely elastic case, Eq. (28) is used to correct the *wave velocity* (c_0) for geometric dispersion effects. In this work we will confine ourselves to the first mode only. Fig. 1a shows a plot of the dimensionless wave velocity ($c(\omega)/c_0$) as a function of the dimensionless wavenumber ($\mathrm{Re}[k'a/2\pi] = a/\lambda$ with λ being the wavelength) for a range of Poisson's ratios. Notice that the dimensionless velocity is expressed in terms of the real parts of the wavenumber of the cylindrical rod and slender bar. The wavenumber for the slender bar is defined in Eqs. (10)–(12). The wavenumber for the cylindrical rod can thus be defined accordingly as

$$k = \frac{\omega}{c} - \mathrm{i}\alpha \approx k'(1 - \mathrm{i}\delta_k). \tag{30}$$

Therefore, from Eqs. (10) or (12) and (30), along with Eq. (28) it is possible to determine the correction for geometric dispersion, in the velocity of low loss viscoelastic rods.

Eqs. (29) and (30) are used to correct the attenuation (α_0) for geometric dispersion in low loss viscoelastic rods. The account for geometric dispersion also yields the leading order term for the attenuation. This is done by considering the imaginary parts of the wavenumbers for the slender bar and the cylindrical rod. Fig. 1b shows the dimensionless attenuation plotted as a function of the dimensionless wavenumber for a range of Poisson's ratios. It is interesting to note that for the first mode, the correction for the attenuation is actually larger than that for the wave velocity. The signal to noise ratio for attenuation measurements is much lower than for velocity measurements. Therefore, as will be shown later, for low loss viscoelastic materials, corrections for attenuation have a very small (often negligible) effect on the actual attenuation data.

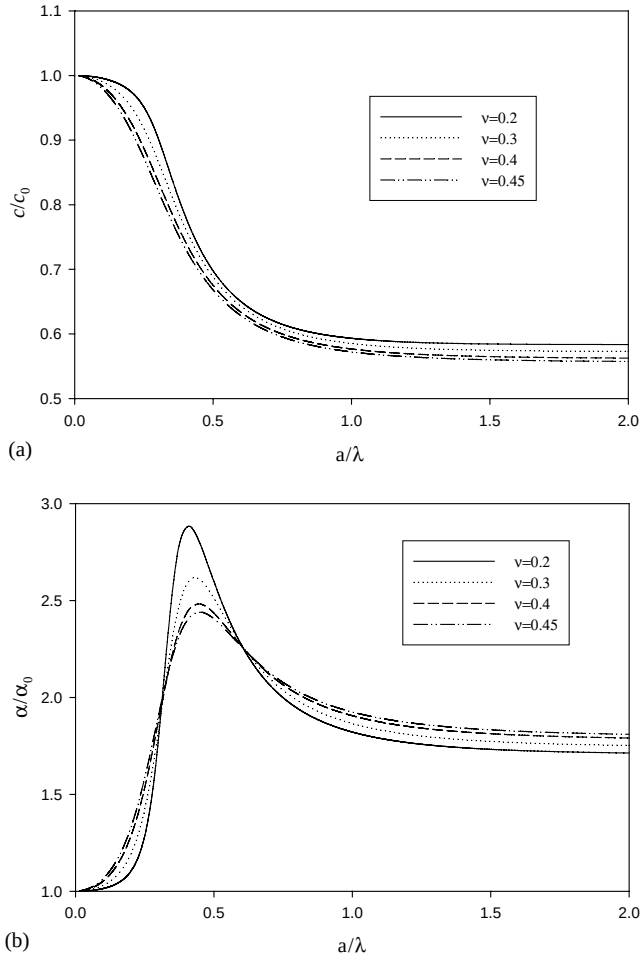

Fig. 1. (a) Dimensionless velocity for first longitudinal mode for a range of Poisson's ratios; determined using simplified Pochhammer frequency equation for low loss viscoelastic material. The ratio $a/\lambda = \mathrm{Re}[k'a/(2\pi)]$. (b) Dimensionless attenuation for first longitudinal mode for a range of Poisson's ratios; determined using simplified Pochhammer frequency equation for low loss viscoelastic material.

2.3. Example: a comparison of the direct and simplified solutions of the frequency equation

Consider a cylindrical rod with *known moduli* that is subjected to a pressure or strain pulse at one end. In this case, as was suggested by Zhao and Gary (1995), it is possible to use the complex Pochhammer frequency equation (see Eq. (1)) *directly* to determine the corrections for geometric dispersion in the wave velocity and attenuation, and construct plots like those shown in Figs. 1a and b. Of course, to use this approach one must know the moduli over the whole frequency range of interest, including material

dispersion effects. An example follows to compare our simplified approach with the above-mentioned direct approach.

Consider a viscoelastic material with the following dynamic moduli: $E' = 5$ GPa, $\tan\delta = 0.05$ or $E'' = 0.25$ GPa. Assume that the moduli do not vary with respect to frequency. For this material it is possible to solve for the first mode of wave propagation in the rod by finding the complex roots of the Pochhammer frequency equation directly. The resulting dependences for c/c_0 and α/α_0 on a/λ are found to be identical to those shown in Figs. 1a and b. This result shows that for materials with $\tan\delta = 0.05$ and a wide range of Poisson's ratios, the simplified Pochhammer equation gives identical results to those found from direct analysis of the complex Pochhammer frequency equation. The main advantage of the present simplified approach is that the moduli of the material need not be determined a priori to apply and use the corrections, as shown in the appendix.

A similar approach can be used to determine the effects of increasing the loss tangent on the simplified Pochhammer frequency equation. Figs. 2a and b show plots of the dimensionless wave velocity and attenuation respectively for a fixed Poisson's ratio of 0.3 and a range of loss tangents. Comparing Figs. 1a and 2a shows that even for very large loss tangents ($\tan\delta \geqslant 0.2$) the effect on the dimensionless wave velocity is very small. Comparing Figs. 1b and 2b shows that the effect of changing the loss tangent on attenuation is also small especially when $\tan\delta \leqslant 0.2$.

At first sight it may be surprising that the approximation that was developed for low loss viscoelastic material is so good even for materials with relatively high loss tangents ($\tan\delta \geqslant 0.2$). However, this becomes clearer when the error in the approximation of the moduli is considered as follows:

$$\frac{E_{\text{approximate}}}{E} = \frac{E'(1+\mathrm{i}\delta)}{E'(1+\mathrm{i}\tan\delta)} = \frac{(1+\delta\tan\delta)+\mathrm{i}(\delta-\tan\delta)}{1+\tan^2\delta}. \tag{31}$$

Using series expansion, and neglecting terms smaller than $O(\delta^4)$ we obtain

$$\frac{E_{\text{approximate}}}{E} \approx 1 - \frac{\delta^4}{3} - \mathrm{i}\,\frac{\delta^3}{3}. \tag{32}$$

Eq. (32) indicates that the error in approximating the real part of the equation is very small, and the error in approximating its imaginary part is only slightly larger. This corresponds with the results shown in Figs. 2a and b.

2.4. Determination of phase velocity and attenuation

Assuming that a cylindrical rod can be regarded as being slender, the phase velocity and attenuation can be determined from measuring strain pulses that travel through the rod (Kolsky, 1963; Bacon, 1998). When a stress or strain pulse propagates in a semi-infinite slender rod, the Fourier transform of the strain $\bar{\varepsilon}$ as a function of the axial coordinate x allows us to find the attenuation and phase velocity from the following

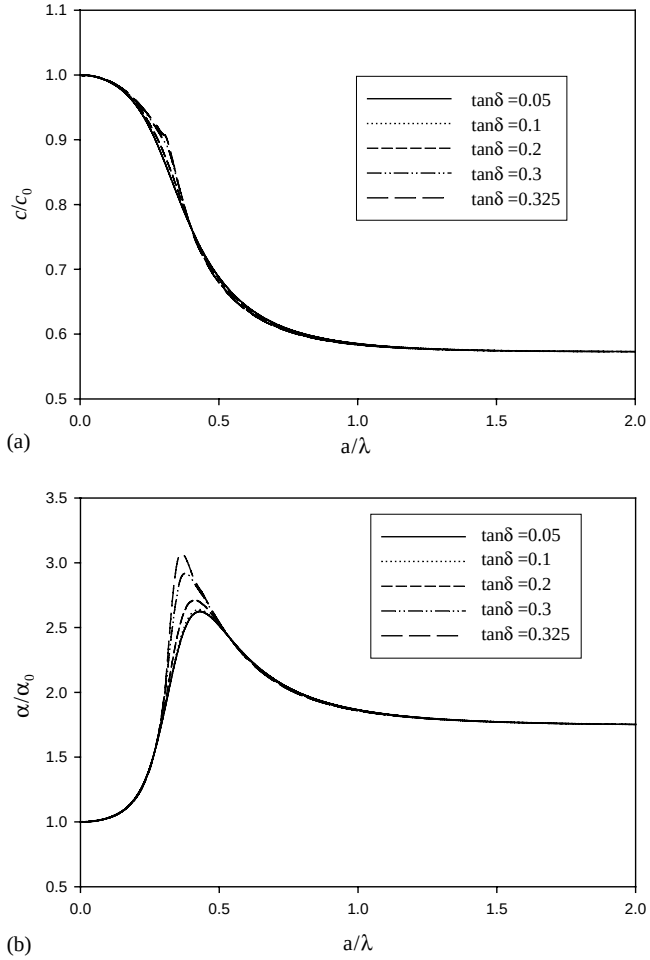

Fig. 2. (a) Dimensionless velocity for viscoelastic material with known storage modulus ($E' = 5$ GPa) and Poisson's ratio (0.3) for a range of loss tangents; determined through finding complex roots of Pochhammer frequency equation. (b) Dimensionless attenuation for viscoelastic material with known storage modulus ($E' = 5$ GPa) and Poisson's ratio (0.3) for a range of loss tangents; determined through finding complex roots of Pochhammer frequency equation.

relations (Sogabe and Kishida, 1982; Lundberg and Blanc, 1988; Blanc, 1993):

$$\alpha(\omega) = -\frac{1}{x_2 - x_1} \ln\left(\frac{|\bar{\varepsilon}(x_2, \omega)|}{|\bar{\varepsilon}(x_1, \omega)|}\right), \tag{33}$$

$$c(\omega) = -\omega \frac{x_2 - x_1}{\theta(x_2, \omega) - \theta(x_1, \omega)}. \tag{34}$$

Notice that with this method using a pulse with a wide frequency content (like a square pulse) enables determination of the attenuation and phase velocity for a range of frequencies.

3. Experiments

3.1. Experimental setup

To measure the wave velocity and attenuation in commercial PMMA over a wide range of frequencies, instrumented rods were prepared and set up as shown in Fig. 3. Rods with nominal length of 70 cm and diameters of 12 and 6.4 mm were used. The strain pulses were measured using Kyowa (0.2 mm gage length, Model KFG-02-120-C1-11) foil resistance strain gages, which were bonded using epoxy at distances of 10 and 35 cm from the impacted end (see Fig. 3). As suggested by Kolsky (1976), small strain gages were used and the adhesive thickness layer was minimized. The strain gage signals were recorded using 12 bit digital conversion of a Nicolet 490 digital oscilloscope, with sampling rate of 5 MHz.

A compressive strain pulse was applied to the rod end by using an air gun to fire PMMA projectiles that were of the same diameter as the rod being tested and 1 cm in length. To minimize friction the rods were supported by polytetrafluoroethylene (PTFE) bushings. For selected experiments using rods of both 12 and 6.4 mm diameter, strain gages (Kyowa 0.2 mm gage length, Model KFG-02-120-C1-11) were placed in both the axial and circumferential directions at the 35 cm position (see Fig. 3). This enabled simultaneous measurement of the axial and circumferential strains and it was used to find Poisson's ratio for both diameter rods.

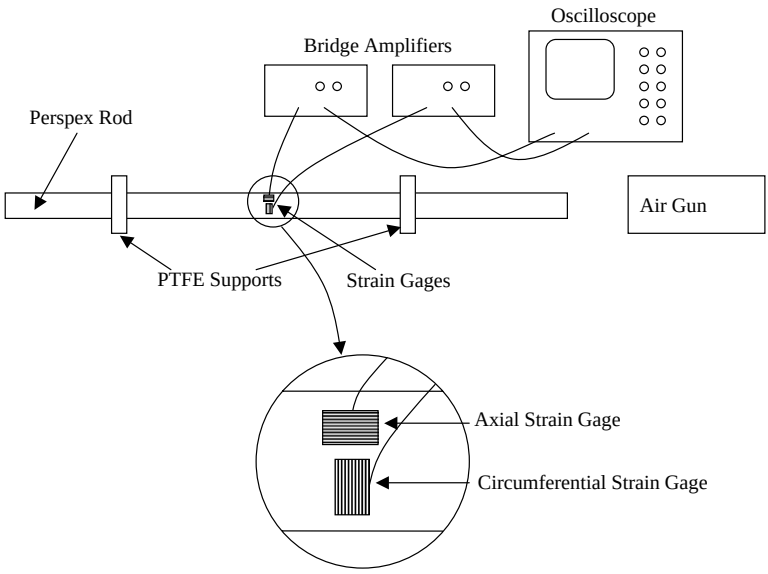

Fig. 3. Experimental setup for phase velocity and attenuation measurement and for measurement of Poisson's ratio.

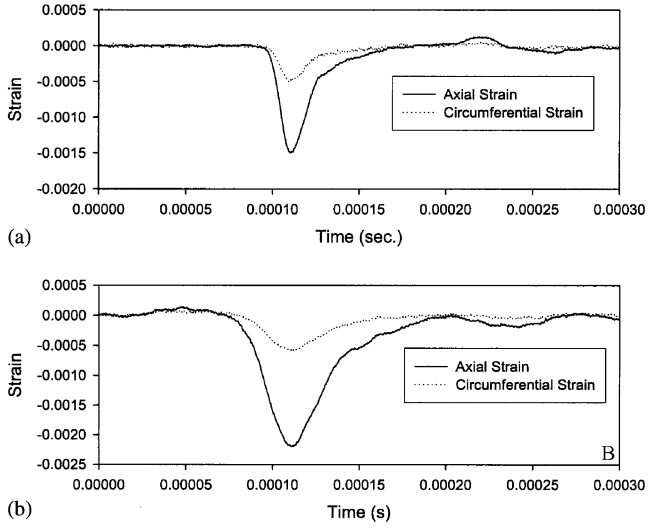

Fig. 4. Measured axial and circumferential strain pulses for PMMA rods that are 6.4 mm in diameter (a) and 12 mm in diameter (b).

3.2. Experimental results

3.2.1. Determination of Poisson's ratio

Fig. 4 shows typical strain pulses that were recorded for rods of both 6.4 and 12 mm diameters. The axial and circumferential strain pulses appear to be in phase, which indicates that Poisson's ratio is real.

Poisson's ratio was determined as a function of frequency by taking the Fourier transform of the strain data. Prior to taking the Fourier transform, the strain data was padded with zeros to increase the number of data points from the original 2048 to 8192, which increases the resolution in the frequency domain. Then the discrete Fourier transform (DFT) was calculated. Phase unwrapping was used to get a continuous function of the phase with respect to frequency. The magnitude and phase of the DFT of the strain pulses from Fig. 4 for the 6.4 and 12 mm diameter rods were obtained as well. The increase in signal attenuation with frequency along with the lower signal to noise ratio for the circumferential strain required limiting the frequency range to 50 kHz for the 6.4 mm diameter rod and to 20 kHz for the 12 mm diameter rod. These show that the phase difference between the axial and circumferential pulses is zero for all frequencies. Fig. 5 shows the average of the real and imaginary parts of Poisson's ratio for the 6.4 mm rods as determined from five separate tests. Also shown in Fig. 5 are the calculated data points from each test, which shows that there is excellent repeatability between the tests. Similarly, Fig. 6 shows several sets of data and their average value for the real and imaginary parts of Poisson's ratio for the 12 mm rod. Notice that the results for both rods are very similar, and they show that Poisson's ratio has just a real part, as was assumed earlier. It varies between 0.25 and 0.3, which is lower than values determined from low-frequency measurements (Ferry, 1980).

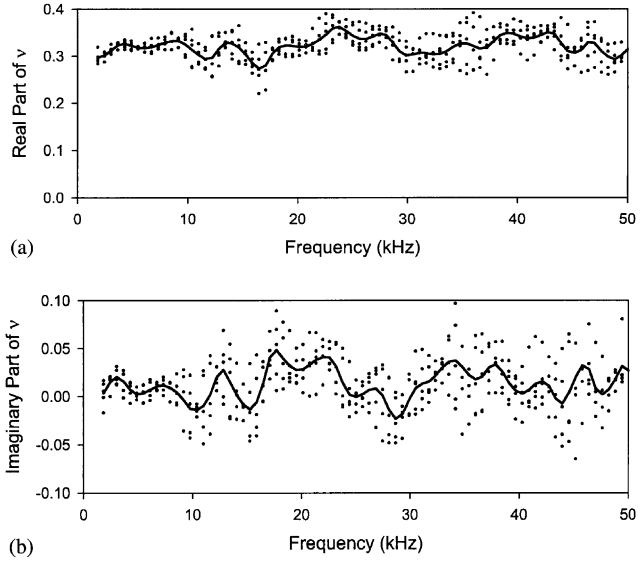

Fig. 5. Real (a) and imaginary (b) parts of Poisson's ratio for the 6.4 mm diameter rod.

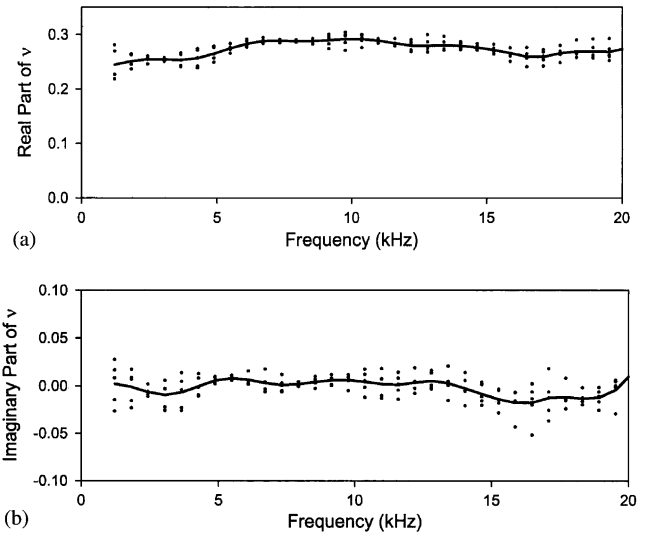

Fig. 6. Real (a) and imaginary (b) parts of Poisson's ratio for the 12 mm diameter rod.

3.2.2. Determination of phase velocity and attenuation

The PMMA rods were impacted at one end, and the traveling strain pulse was measured at two locations, at 10 cm from the impacted end and in the middle of the rod (35 cm from the impacted end). The slender bar model was used to calculate

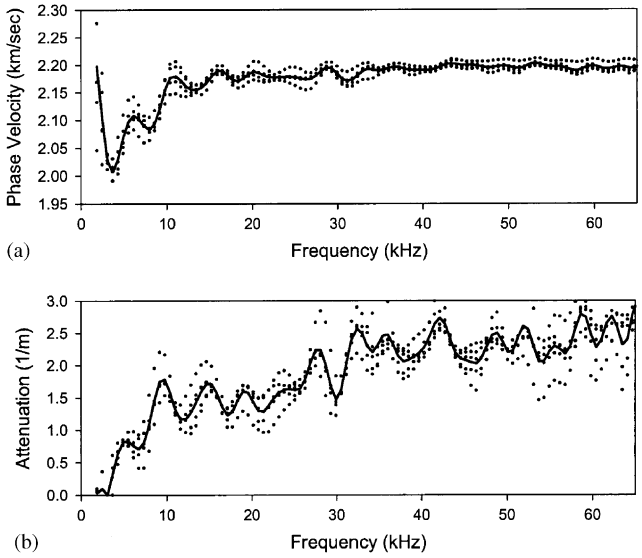

Fig. 7. Calculated phase velocity (a) and attenuation (b) using slender rod model for 6.4 mm diameter rod.

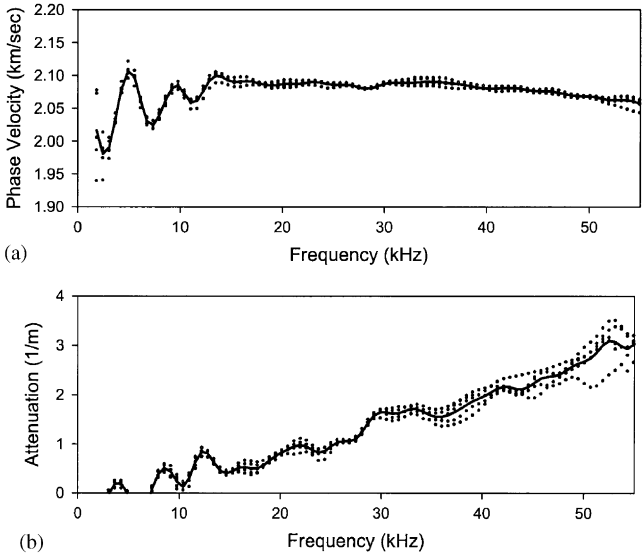

Fig. 8. Calculated phase velocity (a) and attenuation (b) using slender rod model for 12 mm diameter rod.

the attenuation and phase velocity (Eqs. (33) and (34)). Figs. 7 and 8 show the phase velocity and attenuation as determined from five measurements along with the averages for the 6.4 and 12 mm rods, respectively. The attenuation results for both rods are very similar and show more scatter than the phase velocity, because the signal to noise ratio

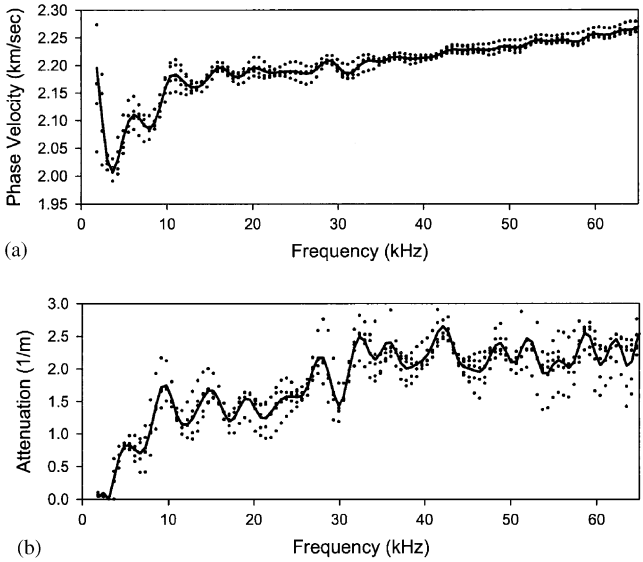

Fig. 9. Calculated phase velocity (a) and attenuation (b) of 6.4 mm diameter rod after correcting for geometric dispersion.

for the magnitude of the strain pulses is lower than for the phase. The phase velocity for both rods is similar at the lower frequencies range with the smaller diameter rod having a slightly higher phase velocity. Since these rods were extruded, it is expected that the smaller diameter rod would have slightly higher molecular orientation in the axial direction (Bacon, 1998). Fig. 7 shows that the phase velocity of the 6.4 mm diameter rod increases initially with frequency, as would be expected. However, the phase velocity reaches a plateau value at a frequency of 35 KHz. For the 12 mm rod, the phase velocity levels off at about 20 KHz, and then decreases with increasing frequency above 30 KHz. As the phase velocity is expected to increase with frequency, both the stabilization and the decrease of this parameter are clear manifestations of geometric dispersion (see e.g., Bacon, 1998).

Correcting for geometric dispersion in this case is possible by using the simplified Pochhammer equation for low loss viscoelastic materials. As was shown in Figs. 5 and 6 Poisson's ratio for these materials varies between 0.25 and 0.3. To simplify the correction procedures, a constant Poisson's ratio of 0.3 was assumed. Figs. 9 and 10 show the phase velocity and attenuation for the rods after correcting for geometric dispersion. Comparing Figs. 7 and 8 and Figs. 9 and 10 shows that the effect of the correction on the phase velocity and attenuation is appreciable for the two investigated diameters. For the smaller rod, the range of useful frequencies extends to about 65 kHz. For the larger diameter rod, the range of frequencies extends to about 55 kHz. After the correction, the phase velocity for the 12 mm rod shows the same trend as the 6.4 mm rod with slightly lower values. Although the magnitude of the correction is

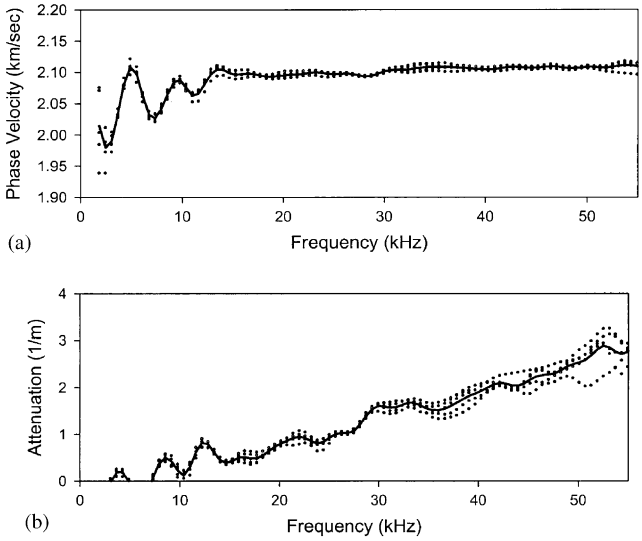

Fig. 10. Calculated phase velocity (a) and attenuation (b) of 12 mm diameter rod after correcting for geometric dispersion.

greater for the attenuation (see Fig. 1b), its effect is small due to the greater scatter in the attenuation results.

4. Discussion

During the propagation of strain or stress pulses in viscoelastic rods, both material and geometric dispersion are possible when the diameter of the rod is of the same order as the wavelength in the material. In the case of elastic rods, the Pochhammer frequency equation can be used to correct for geometric dispersion. For viscoelastic rods, the parameters in the Pochhammer frequency equation are complex making it very difficult or impossible to correct for geometric dispersion without knowing the moduli and Poisson's ratio for the material. In this work, we simplified the Pochhammer frequency equation for low and intermediate loss viscoelastic materials and formulated corrections for geometric dispersion for both the phase velocity and attenuation. The simplified approach requires only approximate values of Poisson's ratio, which is assumed to be real. A fictitious viscoelastic material with known properties was used to compare corrections using the complex Pochhammer frequency equation with the simplified version. It was shown that the simplified Pochhammer frequency equation could be used for materials with fairly large loss tangent (as high as 0.2 or 0.25) with negligible errors. This approach for correcting for geometric dispersion was then experimentally verified with measurements of the phase velocity and attenuation in PMMA rods that are 12 mm in diameter and 6.4 mm in diameter. Without correcting for geometric dispersion, the usable frequency range for determining the phase velocity

and attenuation for the 12 mm rod is about 20 kHz and for the 6.4 mm rod it is about 35 kHz. Using the correction procedure developed here, it was possible to accurately determine the phase velocity and attenuation of the 6.4 mm diameter rod to about 65 kHz, and about 55 kHz for the 12 mm rod.

This result clearly demonstrates the benefit of our simplified approach to the straightforward assessment of the material properties of many viscoelastic materials over a wide frequency range.

5. Conclusions

A simplified approach to solving the Pochhammer frequency equation for viscoelastic materials has been presented. The method relies on separating the equation into real and imaginary parts. These parts are solved separately, rather than being solved frontally for complex moduli that must be known beforehand. In the present method, a preliminary estimate of Poisson's ratio is all that is necessary to determine the viscoelastic properties of a material over a wide range of frequencies.

The experiments are simple to perform and consist of recording (large frequency content) pulse shapes along a viscoelastic bar at two separate locations.

The solution of the viscoelastic frequency equation with the proposed method extends considerably the range of useful frequencies over which the viscoelastic properties are to be determined.

Good agreement with results obtained from the full Pochhammer frequency equation is obtained for the first mode of wave propagation and materials with loss tangent $\tan(\delta) \leqslant 2$.

Acknowledgements

This work was funded in part by the Lady Davis Fellowship Trust at Technion, Israel Institute of Technology.

Appendix A. Correcting for geometric dispersion from wave propagation measurements on a bar

From wave propagation measurements on a bar using strain gages at x_1 and x_2 one can determine the attenuation α_0 and phase velocity c_0, assuming firstly a slender bar (Eqs. (33) and (34)).

However, since the actual bar is not slender, the resulting attenuation and phase velocity include geometric dispersion effects. From Eq. (28), one can calculate the real part of the wavenumber for the bar (including geometric dispersion), and the corresponding dimensionless wavenumber $\mathrm{Re}[k'a/2\pi] = a/\lambda$.

Fig. 1, or Eq. (28), is used to find the corresponding dimensionless wave velocity c/c_0. One thus calculates the corrected phase velocity for a slender bar, thereby

correcting for the geometric dispersion in the actual bar:

$$c_{0\_\text{slender}} = \frac{c_0}{(c/c_0)}, \tag{A.1}$$

where c_{0_slender} is the corrected phase velocity (i.e. the phase velocity for a slender bar of the same viscoelastic material) as determined from measurements with the real (non-slender) bar. Similarly, one uses Fig. 2 or Eq. (29) to find the dimensionless attenuation α/α_0. One then calculates the corrected attenuation for a slender bar, thereby correcting for the geometric dispersion in the actual bar:

$$\alpha_{0\_\text{slender}} = \frac{\alpha_0}{(\alpha/\alpha_0)}, \tag{A.2}$$

where $\alpha_{0\_\text{slender}}$ is the corrected attenuation (i.e. the attenuation for a slender bar of the same viscoelastic material) as determined from measurements with the real (non-slender) bar.

Example. Consider one point for the phase velocity for the 12 mm diameter rod at 50 kHz where $c_0 = 2068$ m/s (Fig. 8a). Then,

$$\text{Re}\left[\frac{k'a}{2\pi}\right] = \frac{\omega a}{2\pi c} = \frac{a}{\lambda} = \frac{50,000a}{c} = 0.145.$$

From Fig. 1a, assuming $v = 0.3$, $c/c_0 = 0.9785$ so that

$$c_{0\_\text{slender}} = \frac{2068 \text{ m/s}}{0.9785} = 2113 \text{ m/s}.$$

Similarly, from Fig. 1b, the attenuation for the 12 mm diameter rod at 50 kHz is $\alpha_0 = 2.683$ 1/m. From Fig. 1b, assuming $v = 0.3$, then $\alpha/\alpha_0 = 1.0755$, so that

$$\alpha_{0\_\text{slender}} = \frac{2.683 \text{ 1/m}}{1.0755} = 2.495 \text{ 1/m}.$$

References

Achenbach, J.D., 1987. Wave Propagation in Elastic Solids. Elsevier Science Publishing Company, New York, pp. 123, 236–240, 242–246.

Bacon, C., 1998. An experimental method for considering dispersion and attenuation in a viscoelastic Hopkinson bar. Exp. Mech. 38, 242–249.

Bancroft, D., 1941. The velocity of longitudinal waves in cylindrical bars. Phys. Rev. 59, 588–593.

Blanc, R.H., 1993. Transient wave propagation methods for determining the viscoelastic properties of solids. J. Appl. Mech. 60, 763–768.

Chree, C., 1889. The equations of an isotropic solid in polar and cylindrical coordinates, their solutions and applications. Trans. Cambridge Philos. Soc. 14, 250–369.

Christensen, R.M., 1982. Theory of Viscoelasticity: an Introduction, 2nd Edition. Academic Press, New York, pp. 21–27.

Coquin, G.A., 1964. Attenuation of guided waves in isotropic viscoelastic materials. J. Acoust. Soc. Am. 36, 1074–1080.

Davis, R.M., 1948. A critical study of the Hopkinson pressure bar. Philos. Trans. R. Soc. London Ser. A 240, 375–457.

Ferry, J.D., 1980. Viscoelastic. Properties of Polymers. Wiley, New York, p. 24.

Graff, K.F., 1975. Wave Motion in Elastic Solids. Clarendon Press, Oxford, p. 470.

Hildebrand, F.B., 1976. Advanced Calculus for Applications. Prentice-Hall, New Jersey, p. 142.

Hillstrom, L., Mossberg, M., Lundberg, B., 2000. Identification of complex modulus from measured strains on axially impacted bar using least squares. J. Sound Vib. 230 (3), 689–707.

Hudson, G.E., 1943. Dispersion of elastic waves in solid circular cylinders. Phys. Rev. 63, 46–51.

Kolsky, H., 1956. The propagation of stress pulses in viscoelastic solids. Philos. Mag. 1, 693–710.

Kolsky, H., 1963. Stress Waves in Solids. Dover Publications, New York, pp. 59–60.

Kolsky, H., 1976. Experimental results of stress wave investigations. In: Mandel, J., Brun, L. (Eds.), Mechanical Waves in Solids. Springer, New York.

Lundberg, B., Blanc, R.H., 1988. Determination of mechanical material properties from the two-point response of an impacted linearly viscoelastic rod specimen. J. Sound Vib. 126, 97–108.

Onoe, M., McNiven, H.D., Mindlin, R.D., 1962. Dispersion of axially symmetric waves in elastic rods. J. Appl. Mech. 29, 729–734.

Pochhammer, L., 1876. Über die fortplanzungsgeschwindigkeiten schwingungen in einem unbegrentzten isotropen kreiscylinder. J. für die reine angewandte Mathematik 81, 324–336.

Sogabe, Y., Kishida, K., 1982. Wave propagation analysis for determining the dynamic properties of high damping alloys. Bull. JSME 25, 321–327.

Sogabe, Y., Tsuzuki, M., 1986. Identification of the dynamic properties of linear viscoelastic materials by the wave propagation testing. Bull. JSME 29, 2410–2417.

Zhao, H., Gary, G., 1995. A three dimensional analytical solution of the longitudinal wave propagation in an infinite linear viscoelastic cylindrical bar. Applications to experimental techniques. J. Mech. Phys. Solids 43, 1335–1348.